Laboratory for Computational Proteomics

www.FenyoLab.org

E-mail: Info@FenyoLab.org

Facebook: *NYUMC Computational Proteomics Laboratory*

Twitter: *@CompProteomics*

International Journal of Mass Spectrometry and Ion Processes, 100 (1990) 63–76
Elsevier Science Publishers B.V., Amsterdam

RADIAL VELOCITY DISTRIBUTIONS OF SECONDARY IONS EJECTED IN ELECTRONIC SPUTTERING OF ORGANIC SOLIDS

D. FENYÖ, A. HEDIN, P. HÅKANSSON and B.U.R. SUNDQVIST

Division of Ion Physics, Department of Radiation Sciences, Uppsala University, Box 535, S-751 21 Uppsala (Sweden)

(Received 5 March 1990)

ABSTRACT

Initial radial velocity distributions of large organic molecular ions as well as low mass contaminant and fragment ions ejected from a solid by impact of 72.3 MeV $^{127}I^{13+}$ have been measured by deflecting the secondary ions by means of a pair of deflection plates placed in the field-free region of a time-of-flight mass spectrometer. The radial velocity distributions have been studied as a function of the angle of incidence of the primary ion for different masses and charge states of the secondary ions. The results indicate that different ejection mechanisms may be involved, applicable in different regions of the secondary ion mass range.

INTRODUCTION

Electronic sputtering, i.e. ejection of atoms and molecules as a result of energy deposition in the electronic system of the sample by fast heavy ions, of large organic molecules has been studied experimentally and theoretically for several years to elucidate the mechanism of ejection and ionization [1, 2]. The radial velocity distributions of large organic molecular ions measured by Ens and co-workers [3, 4] indicate that the ejection of these cannot be described by a thermal model [5, 6] but can be considered as being caused by an expansion of the solid propagating as a pressure pulse [7] or as a shock wave [8]. Some aspects of these experimental results have recently been reproduced by Mosshammer et al. [9].

In this paper results are presented on radial velocity distributions as a function of the angle of incidence of the primary ion for molecular ions with different masses and in different charge states as well as for low mass contaminant and fragment ions. The results are compared with the predictions of an analytical model due to Johnson et al. [7]. Part of the results have already been published in a preliminary form [10] where they were compared with molecular dynamics simulations [11].

0168-1176/90/$03.50

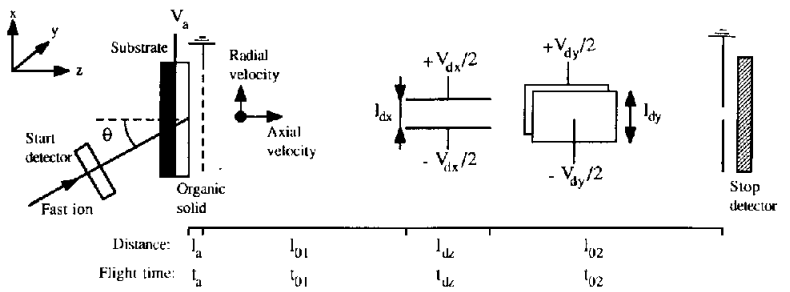

Fig. 1. Experimental set-up.

TABLE 1

Geometrical data (lengths in millimetres) for the two spectrometers used; symbols are defined in Fig. 1

	Spectrometer	
	1	2
l_a	5	5
l_{01}	45	26
l_{dz}	50	30
l_{dy}	39	20
l_{dx}	8	10
l_{02}	300	50
Beam diameter	1	0.25, 1.0
Stop detector diameter	5	1.0, 1.5
Incidence angle	45°	Variable

EXPERIMENTAL

Two different time-of-flight mass spectrometers (Fig. 1, Table 1) were used to identify the ions ejected as a result of the impact of 72.3 MeV $^{127}I^{13+}$ ions from the Uppsala EN-tandem accelerator. In both these spectrometers the primary ions pass through a thin foil detector giving a start pulse for the time to digital converter (TDC). The sample, a thin organic film on a metal backing, is placed at high voltage and thus the ionized ejecta are accelerated towards the grid at ground potential. After passing through the grid the secondary ions enter a region which is field free in an ordinary time-of-flight mass spectrometer. In this region two pairs of deflection plates were placed giving an electric field perpendicular to the spectrometer axis. At the end of the flight tube the secondary ions that passed through a collimator were

detected by a multichannel plate detector and the signal was used as stop signal to the TDC.

If the acceleration voltage is much larger than the initial axial energy, i.e. $qV_a \gg mv_{0z}^2/2$, the time of flight through the spectrometer is given by

$$t_{tot} = t_a + t_{01} + t_{dz} + t_{02} = \sqrt{\frac{m}{2|q|V_a}}(2l_a + l_{01} + l_{dz} + l_{02}) \quad (1)$$

where q is the charge and m is the mass of the ion. The other symbols are defined in Fig. 1. The distance the ion travels perpendicular to the spectrometer axis is obtained from

$$x(t_{tot}) = v_{0x}(t_a + t_{01} + t_{dz} + t_{02}) - \frac{V_{dx}q}{l_{dx}m} t_{dz}\left(\frac{t_{dz}}{2} + t_{02}\right) \quad (2)$$

When rearranged this gives the initial velocity normal to the deflection plates and perpendicular to the spectrometer axis, which will be called radial velocity in this paper although it is the component of the radial velocity along the x axis

$$v_{0x} = \sqrt{\frac{|q|}{2m}} \frac{q}{|q|} \frac{V_{dx} - V_{0d}}{\sqrt{V_a}} \frac{l_{dz} + \Delta l_{dz}}{l_{dx}} \frac{l_{dz}/2 + l_{02}}{2l_a + l_{01} + l_{dz} + l_{02}} \quad (3)$$

where $V_{0d} = -2V_a x(t_{tot})l_{dy}/(l_{dx}(l_{dx}/2 + l_{02}))$ is the voltage needed to make an ion with zero radial velocity component hit the centre of the stop detector and Δl_z is the first order correction to the length of the finite deflection plates [12]

$$\frac{\Delta l_{dz}}{l_{dz}} = \frac{1}{\pi} \cdot \frac{l_{dx}}{l_{dz}} \cdot \left(\sqrt{1 + \left(\frac{l_{dz}}{l_{dy}}\right)^2} - \frac{l_{dz}}{l_{dy}} - \ln\left\{\frac{l_{dx}}{4\pi l_{dz}} \cdot \left[1 + \sqrt{1 + \left(\frac{l_{dz}}{l_{dy}}\right)^2}\right]\right\}\right) \quad (4)$$

The velocity distributions were measured by first maximizing the yield of low mass fragments with the deflection plates in the y direction and then collecting mass spectra for different voltages applied to the deflection plates in the x direction (Figs. 2 and 3). As both the beam spot on the sample and the collimator in front of the stop detector had a finite size the measured velocity distribution $f_m(v_{0x})$ will be related to the initial velocity distribution $f_i(v_{0x}, v_{0y})$ through

$$f_m(v_{0x}) = \int_{-\infty}^{\infty} \int_{-\infty}^{\infty} r(u_x - v_{0x}, u_y - \langle v_{0y}\rangle) f_i(u_x, u_y)\, du_x du_y \quad (5)$$

where $r(v_{0x}, v_{0y})$ is the resolution of the spectrometer which can be calculated from the acceleration voltage and the geometry of the spectrometer.

The samples used were small proteins adsorbed to thin layers of nitrocellulose [13] on either thin aluminium foils or thick silicon slices. The nitrocel-

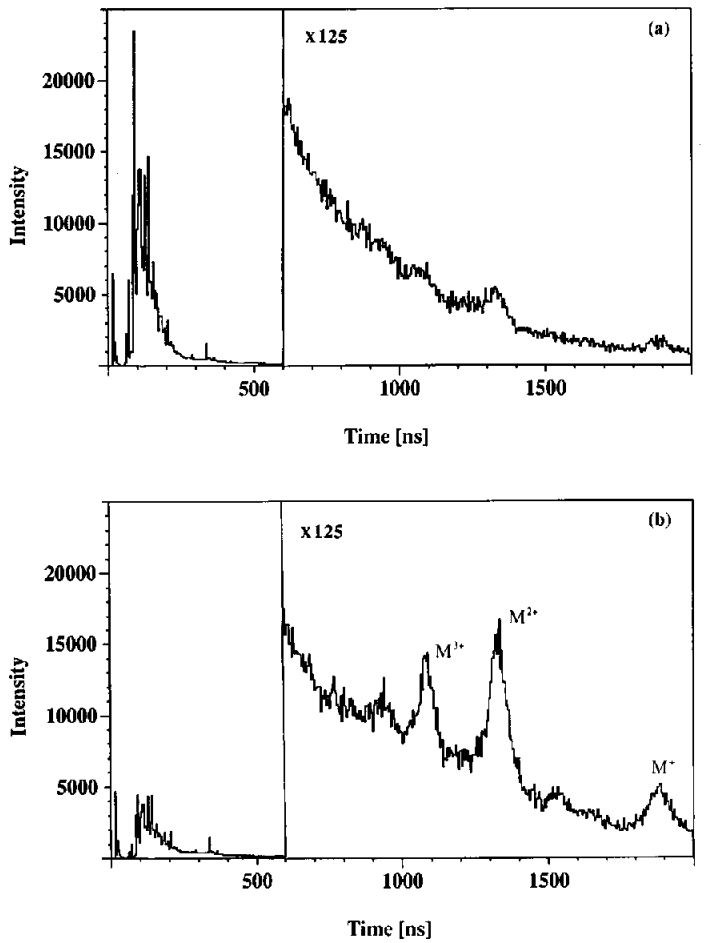

Fig. 2. Time-of-flight spectrum of secondary ions from a sample of PSP adsorbed to nitrocellulose bombarded by 72.3 MeV $^{127}I^{13+}$ from the front at 45° angle of incidence. The voltage difference between the deflection plates in the x direction was +80 V (a) and −60 V (b) giving high yield of fragment ions and molecular ions, respectively.

lulose was electrosprayed or spin coated onto the backings. The proteins were applied either by adsorption from a droplet followed by rinsing to obtain a monolayer coverage of the protein or by spin-drying which gives a multilayer coverage [14]. The proteins used were renin substrate (RS, m = 1801 u), bovine insulin (m = 5734 u), pancreatic sphasholytic peptide (PSP, m = 11 711 u) and porcine trypsin (m = 23 464 u).

The samples of the heavier molecules (insulin, PSP and trypsin) were bombarded from the front at 45° angle of incidence and the samples of RS

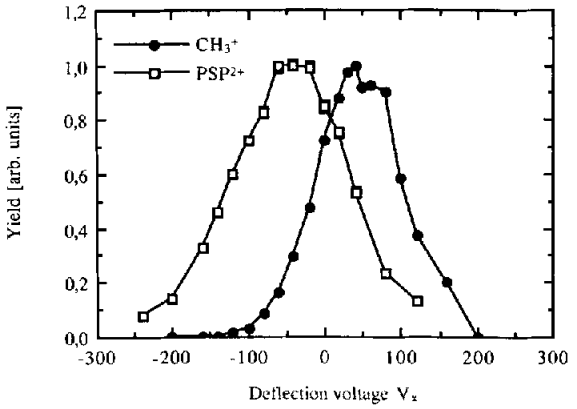

Fig. 3. The yield of CH_3^+ and PSP^{2+} as a function of the voltage difference between the deflection plates in the x direction.

were bombarded from the back at 0°, 10°, 45° and 60° angle of incidence with 72.3 MeV $^{127}I^{13+}$ ions. The spectrometer with variable angle of incidence of the primary ion was carefully aligned to prevent the beam spot from moving as the angle of incidence was changed as this would change V_{0d} and thus the mean radial velocity. The influence on the results from the inhomogeneity of the field between the deflection plates is much smaller than the effects measured and can be neglected. This was tested by measuring the radial velocity distribution of H^+ at different acceleration voltages. The H^+ ions then pass at different distances from the deflection plates and they are affected by different parts of the field.

RESULTS

The initial radial velocity distributions of molecular ions and those of low mass ions behave very differently under variations of the angle of incidence of the primary ion. Thus, they are presented and discussed separately.

Molecular ions

Figure 4 shows the measured radial velocity distributions of positive molecular ions from a multilayer sample of RS for different angles of incidence. For normal incidence the distribution has two peaks and a minimum for zero radial velocity. As the angle of incidence is increased to 10° the relative magnitude of the two peaks changes. For 45° the distribution has only one peak which moves towards zero radial velocity for further increase of the angle of incidence. The protein coverage has only a minor effect on the radial

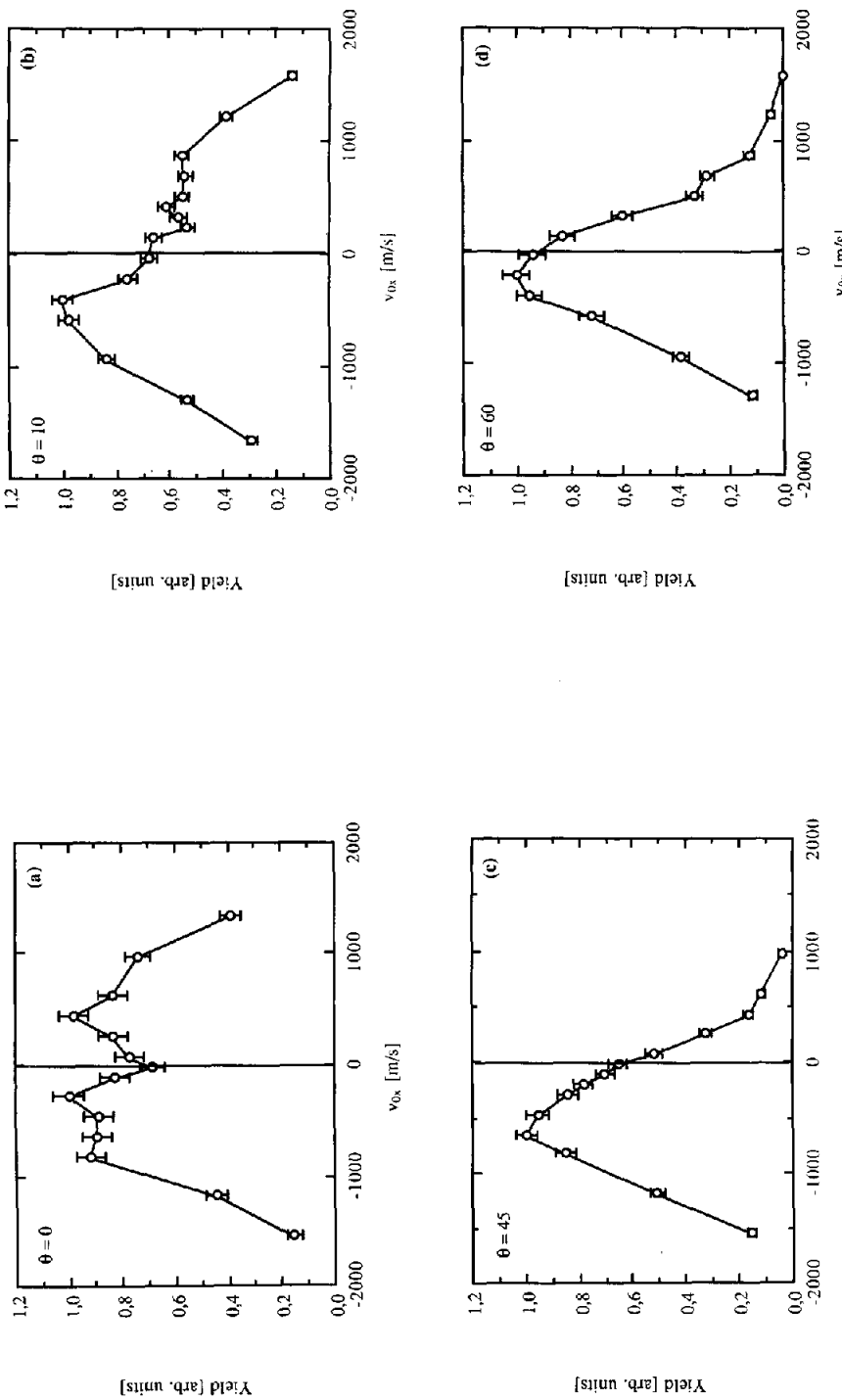

Fig. 4. The radial velocity distribution of the molecular ion of renin substrate (RS^+) for different angles of incidence: (a) 0°; (b) 10°; (c) 45°; (d) 60°.

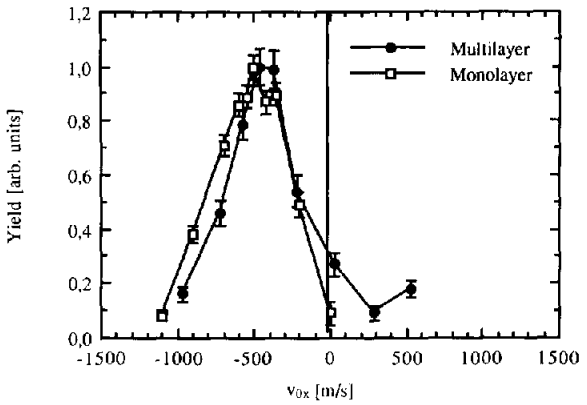

Fig. 5. Radial velocity distribution of singly positively charged molecular ions of bovine insulin for samples with submonolayer and multilayer protein coverage prepared with the adsorption-rinsing and the spin-drying technique, respectively.

velocity distribution at 45° angle of incidence as shown in Fig. 5 for molecular ions of bovine insulin from a monolayer and a multilayer sample. Radial velocity distributions for molecular ions of bovine insulin, PSP and porcine trypsin in different charge states are presented in Fig. 6. For PSP and porcine trypsin the mean radial velocity is larger for higher charge state (Fig. 6cd). The resolution of the method decreases for increasing charge state giving broader distributions, but this effect is much smaller than the measured broadening of the distributions for higher charge states. This increase in mean radial velocity for higher charge states is very small for bovine insulin (Fig. 6ab). In Fig. 7 the mean radial energy is shown as a function of mass for 45° angle of incidence.

Low mass contaminant and fragment ions

While the radial velocity distribution of the molecular ions shows a strong dependence on the angle of incidence, the same dependence for low mass contaminant and fragment ions (CH_3^+, H_2O^+, H_3O^+, Al^+, NO^+) is within the errors of our measurements. Exceptions are the radial velocity distributions of H^+ and H_2^+ which are slightly shifted when the angle of incidence is changed from 0° to 45° (Figs. 8 and 9).

The FWHM of the initial radial velocity distributions were calculated by a least-squares fit of Eq. 5 to the experimental data assuming the initial radial velocity distribution to be Gaussian. The resolution $r(v_{0x}, v_{0y})$ was calculated from the geometry of the spectrometer taking into account the broadening of the beam due to multiple scattering in the start detector [15]. Figure 10 shows

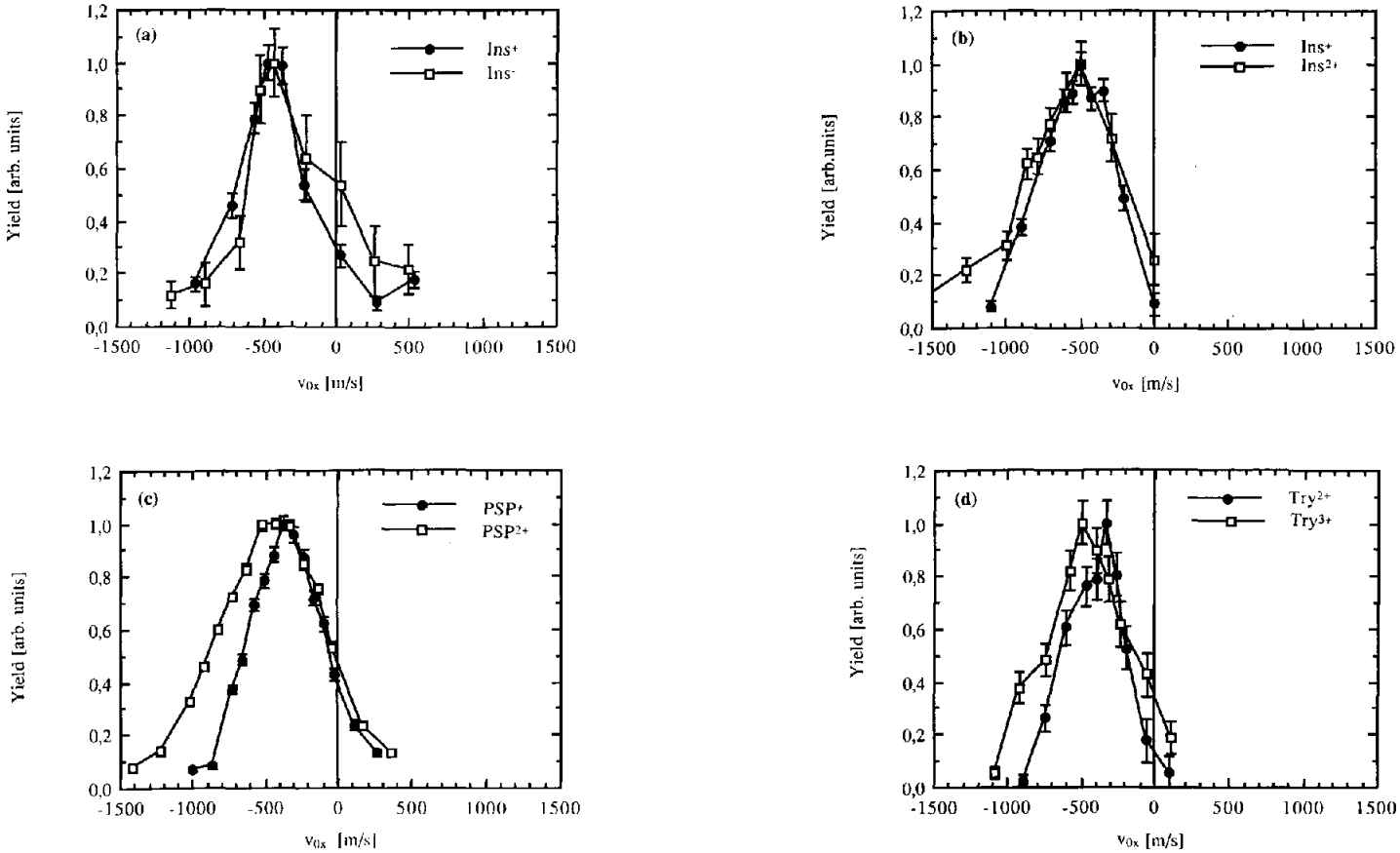

Fig. 6. Radial velocity distribution of molecular ions in different charge states: (a) bovine insulin singly negatively and singly positively charged; (b) bovine insulin 1+, 2+; (c) PSP 1+, 2+; (d) porcine trypsin 2+, 3+.

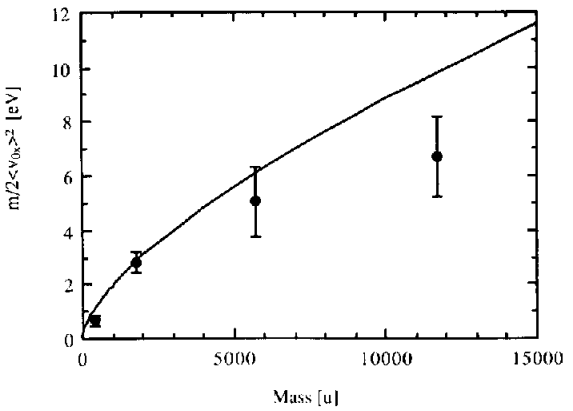

Fig. 7. Mean radial velocity of singly charged molecular ions as a function of the molecular ion mass. The solid line is the explicit mass dependence of Eq. 6 normalized to the experimental data point of RS (m = 1801 u).

two measurements of the radial velocity distribution of the fragment ion CH_3^+ for normal incidence with different collimators in front of the start and stop detectors, i.e. the resolution $r(v_{0x}, v_{0y})$ was varied. The FWHM of the initial radial velocity distributions in the two measurements obtained from the least squares fit differ by less than 5%. The energy corresponding to the FWHM of the radial velocity distribution was approximately constant as a function of mass (Fig. 11) for all low mass contaminant and fragment ions studied except for H^+ and H_2^+.

DISCUSSION

Molecular ions

The variations of the shape of the initial radial velocity distributions of the molecular ions as a function of the angle of incidence has been reproduced qualitatively by molecular dynamics simulations [10, 11] and analytical models [7, 8]. The shapes of the initial radial velocity distributions of the molecular ions can be described by ejection, from a volume with low energy density, by the pressure pulse which is emitted from the cylindrical volume energized by the incident ion. According to the analytical model due to Johnson *et al.* [7], where the energy is assumed to diffuse or propagate as a sharp pulse in a half space where initially the energy is concentrated along a line, the mean radial impulse of a molecule in the plane of incidence ejected from the surface is given by

$$\langle p_x \rangle \propto m^{5/6} \left\langle \frac{1}{x} \right\rangle \Leftrightarrow \frac{1}{2m} \langle p_x \rangle^2 \propto m^{2/3} \left\langle \frac{1}{x} \right\rangle^2 \tag{6}$$

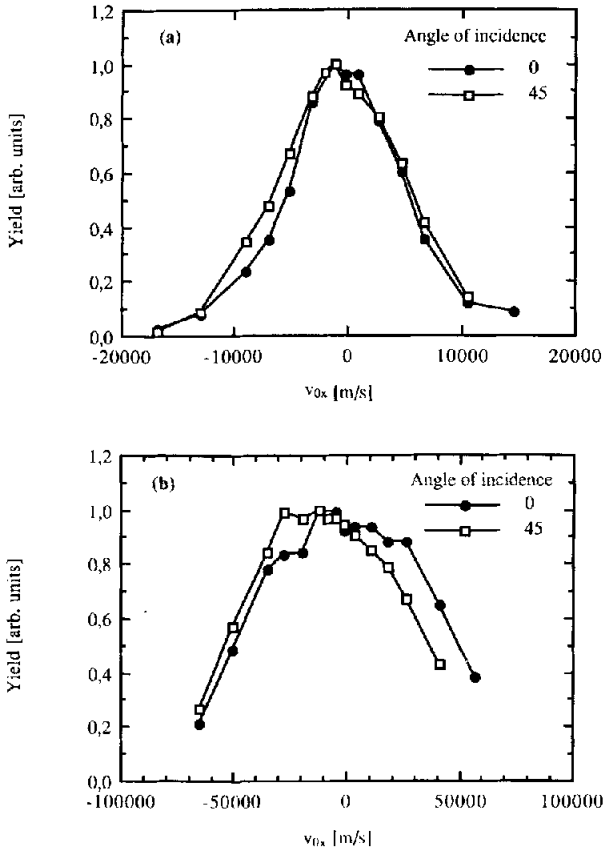

Fig. 8. Radial velocity distribution of the fragment ions: (a) CH_3^+ ; (b) H^+ for 0° and 45° angle of incidence.

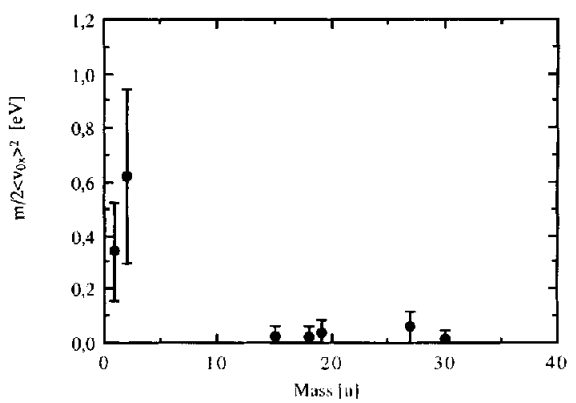

Fig. 9. Mean radial energy for a few fragment ions as a function of mass for 45° angle of incidence.

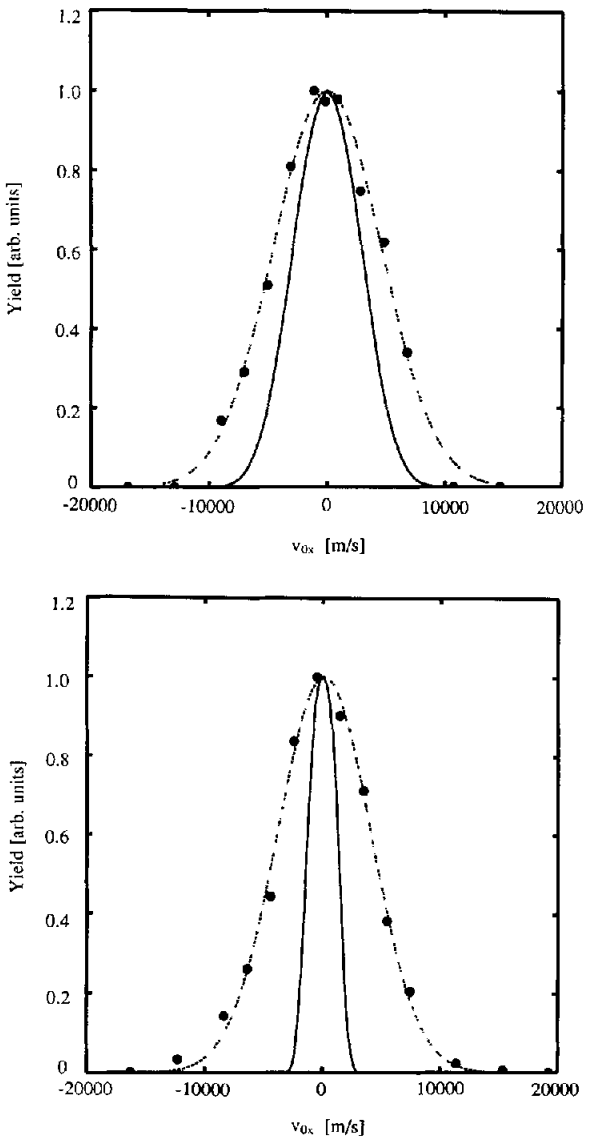

Fig. 10. Two different measurements of the radial velocity distribution of the fragment ion CH_3^+ (points) for normal incidence for two different resolutions (the solid line is $r(v_{0x}, \langle v_{0y} \rangle)$). The dotted lines are the least-squares fit of Eq. 5 to the experimental data assuming a Gaussian initial radial velocity distribution.

where m is the molecular mass and x the distance in the plane of incidence on the sample surface from the point of impact to the ejection site. In the derivation it is assumed that the cohesive energy is proportional to the surface area of the molecule. The average over the distance $\langle 1/x \rangle$ depends on the

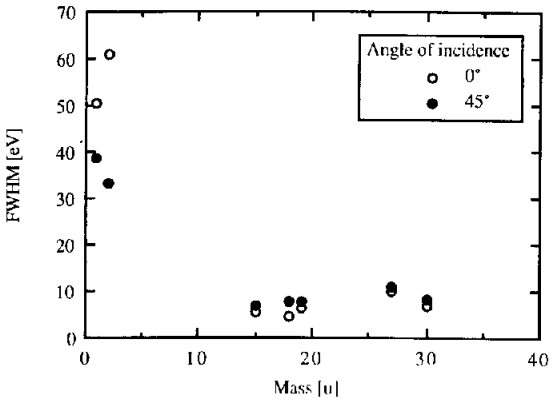

Fig. 11. The energy corresponding to the FWHM of the radial velocity distribution for a few fragment ions as a function of mass. The FWHM of an initial radial velocity distribution was obtained by a least-squares fit of Eq. 5 to the experimental data assuming a Gaussian initial radial velocity distribution.

probability for ejection of an intact ionized molecular ion from a distance x from the point of impact. In the analytical model a part of the solid is considered as ejected if the size of the axial impulse, $p_z \propto m^{5/6}/x(1 - x/|x| \sin\theta)/\cos\theta$ (derived with the same assumptions as the mean radial impulse), is larger than the cohesive forces of the solid. Thus, $\langle 1/x \rangle$ depends on the angle of incidence as the probability of ejection from a distance x will depend on the angle of incidence.

The results presented for molecular ions in this paper can qualitatively be understood using Eq. 6. Increasing the angle of incidence and keeping x constant, p_z will increase for negative x and decrease for positive. The analytical model thus predicts the radial velocity distribution to change qualitatively in the same way as in Fig. 4. Both the relative height of the two peaks and the shift of the peaks in velocity is described by the change in ejection probability. The shift of the radial distribution to lower velocities for larger angle of incidence is due to the fact that molecules are ejected further away from the point of impact and thus attain a lower mean radial velocity. The larger mean radial velocities for molecular ions in higher charge states (Fig. 6) indicate that in this picture the higher charge states are created with a larger probability close to the ion trajectory. The energy density is high close to the ion path and thus multiple ionizations occur more frequently and highly charged possibly pre-formed ions are more easily removed from the surface than in a region with low energy density. It has also been proposed that such a difference in mean radial velocity for different charge states could be caused by repulsion from the positively charged track [16]. However, the lifetime of the charged

track is probably too short to give such a large influence on the heavy molecular ions. In Fig. 7 the explicit mass dependence of Eq. 6 is shown together with the measured mean radial energies for the singly positively charged molecular ions. The curve is normalized to the data point of RS. As $\langle 1/x \rangle$ depends on how large an energy density a molecule can survive (and large molecules are more fragile than small ones), the mean radial velocity increases more slowly than $m^{2/3}$.

Low mass contaminant and fragment ions

The dependence on the angle of incidence of the initial radial velocity distributions for the low mass contaminant and fragment ions, except for the hydrogen clusters is very weak and could not be detected in these experiments (Fig. 8). This indicates that these low mass ions are not ejected in a gas jet as proposed for condensed gases [17]. They may be evaporated from the volume energized by the primary ion [5, 6]. This is also supported by the fact that the width of the energy distributions, which would then correspond to the average temperature in the volume, is nearly independent of the mass and angle of incidence (Fig. 11). The radial velocity distributions of H^+ and H_2^+, on the other hand, depend weakly on the angle of incidence (Fig. 8b,9) and their energy distributions are much broader than those of the other low mass fragments (Fig. 11), which shows that they are neither evaporated from the surface nor ejected in a gas jet, as the shift in velocity is too small and in the wrong direction. Perhaps the ejection of the hydrogen clusters can be explained by repulsion from a short-lived positively charged track [18].

CONCLUSIONS

The experimental results on the initial radial velocity distributions of molecular ions presented here indicate that the heavy molecular ions are ejected from a region with low energy density by the pressure pulse emitted from the expanding high energy density region near the primary ion trajectory. The description of the ejection of low mass fragment and contaminant ions as being evaporation from the volume energized by the primary ion does not contradict the measured radial energy distributions, being nearly independent of the secondary ion mass and the primary ion incidence angle.

REFERENCES

1 B.U.R. Sundqvist, in R. Behrisch and K. Wittmaack (Eds.), Sputtering by Particle Bombardment III, Springer, Berlin, (1990) in press.
2 R.E. Johnson, Int. J. Mass Spectron. Ion Processes, 78 (1987) 357.

3 W. Ens, B.U.R. Sundqvist, A. Hedin, P. Håkansson and G. Jonsson, Phys. Rev. B, 39 (1989) 763.
4 W. Ens, B.U.R. Sundqvist, P. Håkansson, D. Fenyö, A. Hedin and G. Jonsson, J. Phys. (Paris), C2 (1989) 9.
5 R.R. Lucchese, J. Chem. Phys., 86 (1987) 443.
6 H. Voit, E. Nieschler, B. Nees, R. Schmidt, C.H. Schoppmann, P. Beining and J. Scheer, J. Phys. (Paris), C2 (1989) 237.
7 R.E. Johnson, B.U.R. Sundqvist, A. Hedin and D. Fenyö, Phys. Rev. B, 40 (1989) 49.
8 I.S. Bitensky, A.M. Goldenberg and E.S. Parilis, in A. Hedin, B.U.R. Sundqvist and A. Benninghoven (Eds.), Proc. Ion Formation from Organic Solids (IFOS V), Wiley, Chichester, 1990, p. 205.
9 R. Mosshammer, R. Matthäus, K. Wien, Y. LeBeyec and G. Bolbach, in A. Hedin, B.U.R. Sundqvist and A. Benninghoven (Eds.), Proc. Ion Formation from Organic Solids (IFOS V), Wiley, Chichester, 1990, p. 17.
10 D. Fenyő, A. Hedin, P. Håkansson, R.E. Johnson and B.U.R. Sundqvist, in A. Hedin, B.U.R. Sundqvist and A. Benninghoven (Eds.), Proc. Ion Formation from Organic Solids (IFOS V), Wiley, Chichester, 1990, p. 33.
11 D. Fenyő, B.U.R. Sundqvist, B.R. Karlsson and R.E. Johnson, Phys. Rev. B, (1990) in press.
12 A. Recknagel, Z. Phys., 111 (1938) 61.
13 G. Jonsson, A. Hedin, P. Håkansson, B.U.R. Sundqvist, G. Säve, P. Nielsen, P. Roepstorff, K.E. Johansson, I. Kamensky and M. Lindberg, Anal. Chem., 58 (1986) 1084.
14 G. Jonsson, G. Brinkmalm, B.U.R. Sundqvist, A. Hedin and P. Håkansson, TSL-ISV 21, ISSN 0284-2769, internal report, Dept. Radiation Sciences, Uppsala, 1989.
15 J.B. Marion and F.C. Young, Nuclear Reaction Analysis, North-Holland, Amsterdam, 1968.
16 K. Wien, Radiat. Eff. Defects Solids, 109 (1989) 169.
17 U.M. Urbassek and J. Michl, Nucl. Instrum. Methods B 22 (1987) 480.
18 S. Widdiyasekera, P. Håkansson and B.U.R. Sundqvist, Nucl. Instrum. Methods, Part B, 33 (1988) 836.